

# Catalyst-Free Aromatic Nucleophilic Substitution of *meso*-Bromoporphyrins with Azide Anion: Efficient Synthesis and Structural Analyses of *meso*-Azidoporphyrins

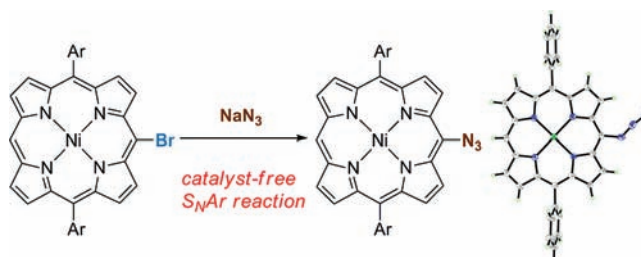
Ken-ichi Yamashita,\* Kazuyuki Kataoka, Motoko S. Asano, and Ken-ichi Sugiura\*

Department of Chemistry, Graduate School of Science and Engineering, Tokyo Metropolitan University, 1-1 Minami-Osawa, Hachioji, Tokyo 192-0397, Japan

\*yamashita-kenichi@tmu.ac.jp; sugiura@porphyrin.jp

Received November 4, 2011

## ABSTRACT



*meso*-Mono- or diazidoporphyrins were readily obtained in high yields by the catalyst-free aromatic nucleophilic reaction of the corresponding bromoporphyrins with azide anions under mild conditions. The molecular structures of the obtained azides were unambiguously determined by X-ray crystallographic analysis.

Functionalization of the porphyrin periphery is one of the most important approaches to achieve the construction of novel porphyrin-based materials with unique chemical, biological, or optical properties derived from

(1) Vicente, M. G. H.; Jaquinod, L. In *The Porphyrin Handbook*; Kadish, K. M., Smith, K. M., Guillard, R., Eds.; Academic Press: San Diego, 2003; Vol. 1, pp 149–199.

(2) For recent examples of nucleophilic reactions which involve porphyrin  $\pi$ -cation radicals, see: (a) Shen, D.-M.; Liu, C.; Chen, X.-G.; Chen, Q.-Y. *J. Org. Chem.* **2009**, *74*, 206–211. (b) Devillers, C. H.; Dime, A. K. D.; Cattey, H.; Lucas, D. *Chem. Commun.* **2011**, 1893–1895.

(3) For recent reviews on nucleophilic reactions with organometallic reagents followed by oxidation, see: (a) Senge, M. O. *Acc. Chem. Res.* **2005**, *35*, 733–743. (b) Senge, M. O. *Chem. Commun.* **2011**, 1943–1960.

(4) For recent examples of nucleophilic reactions with organometallic reagents followed by oxidation, see: (a) Takanami, T.; Wakita, A.; Sawaizumi, A.; Iso, K.; Onodera, H.; Suda, K. *Org. Lett.* **2008**, *10*, 685–687. (b) Takanami, T.; Matsumoto, J.; Kumagai, Y.; Sawaizumi, A.; Suda, K. *Tetrahedron Lett.* **2009**, *50*, 68–70. (c) Takanami, T.; Hayashi, S.; Iso, K.; Matsumoto, J.; Hino, F. *Tetrahedron Lett.* **2011**, *52*, 5345–5348.

(5) For recent reviews on transition-metal-catalyzed coupling reactions of *meso*-haloporphyrins, see: Shinokubo, H.; Osuka, A. *Chem. Commun.* **2009**, 1011–1021.

the extended  $\pi$ -electron system.<sup>1</sup> To date, a wide variety of porphyrins with carbon- or heteroatom-based functional groups have been synthesized through electrophilic substitutions, nucleophilic reactions involving porphyrin  $\pi$ -cation radicals, nucleophilic reactions with organometallic reagents followed by oxidation, or transition-metal-catalyzed coupling reactions.<sup>1–7</sup> In particular, a recent outstanding development of transition metal catalysts

(6) For recent examples of transition-metal-catalyzed C–N bond formations of *meso*-haloporphyrins, see: (a) Takanami, T.; Hayashi, M.; Hino, F.; Suda, K. *Tetrahedron Lett.* **2003**, *44*, 7353–7357. (b) Chen, Y.; Zhang, X. P. *J. Org. Chem.* **2003**, *68*, 4432–4438. (c) Gao, G. Y.; Chen, Y.; Zhang, X. P. *Org. Lett.* **2004**, *6*, 1837–1840. (d) Chen, Y.; Gao, G.-Y.; Zhang, X. P. *Tetrahedron Lett.* **2005**, *46*, 4965–4969. (e) Esdaile, L. J.; McMurtrie, J. C.; Turner, P.; Arnold, D. P. *Tetrahedron Lett.* **2005**, *46*, 6931–6935. (f) Esdaile, L. J.; Senge, M. O.; Arnold, D. P. *Chem. Commun.* **2006**, 4192–4194. (g) Liu, C.; Shen, D. M.; Chen, Q. Y. *J. Org. Chem.* **2007**, *72*, 2732–2736. (h) Sakamoto, R.; Sasaki, T.; Honda, N.; Yamamura, T. *Chem. Commun.* **2009**, 5156–5158. (i) Pereira, A. M. V. M.; Neves, M. G. P. M. S.; Cavaleiro, J. A. S.; Jeandon, C.; Gisselbrecht, J.-P.; Choua, S.; Ruppert, R. *Org. Lett.* **2011**, *13*, 4742–4745.

enabled us to introduce various functional groups in high yields.<sup>6,7</sup> However, several active metal catalysts are expensive or not commercially available.

*meso*-Nitrogen-substituted porphyrins are relatively well-investigated heteroatom-substituted porphyrins because the introduced substituents strongly affect a  $\pi$ -electron system of the porphyrin. There have been two typical synthetic routes to *meso*-nitrogen-substituted porphyrins. One is a transformation of an amino group ( $-\text{NH}_2$ ),<sup>8</sup> which is introduced by a nitration and a subsequent reduction of the introduced nitro group.<sup>9</sup> The other is a transition-metal-catalyzed C–N(amine or amide) bond formation from *meso*-haloporphyrins described above.<sup>6</sup>

Azido groups also play important roles in synthetic chemistry due to their versatile conversion to other functional groups such as amine (by reduction), 1,2,3-triazole (by cycloaddition with alkyne), and highly reactive nitrene (by thermal decomposition or photodecomposition).<sup>10</sup> Despite the synthetic usefulness of the azide groups, there have been few reports directly concerning azido-substituted porphyrins.<sup>11,12</sup> In a previous report, *meso*-azidoporphyrin (Ni complex) was synthesized by treatment of sodium azide with a diazonium salt prepared from *meso*-aminoporphyrin (85% yield).<sup>11b</sup> However, the synthesis of the

*meso*-aminoporphyrins is quite cumbersome as described above. Furthermore, it is quite troublesome to synthesize *meso*-diazidoporphyrin by the reported procedure because of the highly air-sensitive nature of the precursors, i.e., *meso*-diaminoporphyrins.<sup>13</sup> Therefore, there is still plenty of room for improvement in the synthetic route to develop the chemistry of azidoporphyrins. Aromatic nucleophilic substitution ( $\text{S}_{\text{N}}\text{Ar}$ ) reactions of aryl halides with an azide anion are facile and efficient procedures to synthesize aromatic azides, especially in the case of electron-deficient aromatics.<sup>10</sup> However, the  $\text{S}_{\text{N}}\text{Ar}$  reactions of haloporphyrins have not been energetically investigated as a method for peripheral functionalization of the porphyrins.<sup>14</sup> More recently, Balaban et al. reported the practical  $\text{S}_{\text{N}}\text{Ar}$  reactions of *meso*-bromoporphyrins with alkylamines.<sup>14e,f</sup> Herein, we have found that *meso*-mono- or dibromodiarlyporphyrins undergo the  $\text{S}_{\text{N}}\text{Ar}$ -type reaction with an azide anion under mild conditions without any additive to give the corresponding azidoporphyrins in high yields. In addition, we have revealed the first molecular and crystal structures of mono- and diazidoporphyrins, which are, to the best of our knowledge, one of the largest aromatic azides confirmed by X-ray analysis.<sup>15</sup>

First, we investigated a reaction of a Ni(II) complex of *meso*-bromodiarlyporphyrin **1a(Ni)** with sodium azide. Typically, **1a(Ni)** was treated with 10 equiv of sodium azide in DMF under a  $\text{N}_2$  atmosphere with protection from light. When the reaction was performed at 40 °C for 7 h, the desired *meso*-azidoporphyrin **2a(Ni)** was obtained in 93% yield (Table 1, entry 1). The reaction time was reduced by elevating the reaction temperature to 60 °C (entry 2), although a longer reaction time led to the thermal decomposition of **2a(Ni)** into *meso*-aminoporphyrin **3a(Ni)** and undefined brown byproducts (entry 3). At 90 °C, **2a(Ni)** was completely decomposed with the formation of **3a(Ni)** in 25% yield (entry 4). When the amount of sodium azide was reduced to 5 equiv (entry 5), a longer reaction time was required to complete the reaction. Therefore, the yield of **2a(Ni)** was reduced compared to entry 3 (the same condition except for the amount of sodium azide). The reaction proceeded smoothly in DMF while no reaction proceeded in THF (entry 6). Reaction of *meso*-bromodiphenylporphyrin **1b(Ni)** also gave azidoporphyrin **2b(Ni)** in 68% yield (entry 7). Because of the poor solubility of **1b(Ni)** in DMF, a longer reaction time was required.

(13) To the best of our knowledge, *meso*-diaminodiarlyporphyrins and their metal complexes have not been reported.

(14) (a) Baldwin, J. E.; Crossley, M. J.; DeBernardis, J. *Tetrahedron* **1982**, *38*, 685. (b) Gong, L. C.; Dolphin, D. *Can. J. Chem.* **1985**, *63*, 3793–3799. (c) Crossley, M. J.; King, L. G.; Simpson, J. L. *J. Chem. Soc., Perkin Trans. 1* **1997**, 3087–3096. (d) Crossley, M. J.; King, L. G.; Pyke, S. M.; Tansey, C. W. *J. Porphyrins Phthalocyanines* **2002**, *6*, 685–694. (e) Balaban, M. C.; Chappaz-Gillot, C.; Canard, G.; Fuhr, O.; Roussel, C.; Balaban, T. S. *Tetrahedron* **2009**, *65*, 3733–6522. (f) Balaban, M. C.; Eichhöfer, A.; Buth, G.; Hauschild, R.; Szymkowski, J.; Kalt, H.; Balaban, T. S. *J. Phys. Chem. B* **2008**, *112*, 5512–5521.

(15) Cambridge Structural Database (CSD), version 5.3.2 (updated May, 2011).

(7) For recent examples of transition-metal-catalyzed other C–heteroatom or C–C bond formations of *meso*-haloporphyrins, see: (a) Hyslop, A. G.; Kellett, M. A.; Iovine, P. M.; Therien, M. J. *J. Am. Chem. Soc.* **1998**, *120*, 12676–12677. (b) Gao, G.-Y.; Colvin, A. J.; Chen, Y.; Zhang, X. P. *Org. Lett.* **2003**, *5*, 3261–3264. (c) Gao, G.-Y.; Colvin, A. J.; Chen, Y.; Zhang, X. P. *J. Org. Chem.* **2004**, *69*, 8886–8892. (d) Takanami, T.; Hayashi, M.; Chijimatsu, H.; Inoue, W.; Suda, K. *Org. Lett.* **2005**, *7*, 3937–3940. (e) Atefi, F.; McMurtrie, J. C.; Turner, P.; Duriska, M.; Arnold, D. P. *Inorg. Chem.* **2006**, *25*, 6479–6489. (f) Matano, Y.; Shinokura, T.; Matsumoto, K.; Imahori, H.; Nakano, H. *Chem.—Asian J.* **2007**, *2*, 1417–1429. (g) Gao, G. Y.; Ruppel, J. V.; Fields, K. B.; Xu, X.; Chen, Y.; Zhang, X. P. *J. Org. Chem.* **2008**, *73*, 4855–4858. (h) Matano, Y.; Matsumoto, K.; Nakao, Y.; Uno, H.; Sakaki, S.; Imahori, H. *J. Am. Chem. Soc.* **2008**, *130*, 4588–4589. (i) Enakieva, Y. Y.; Bessmertnykh, A. G.; Gorbunova, Y. G.; Stern, C.; Rousselin, Y.; Tsvivadze, A. Y.; Guillard, R. *Org. Lett.* **2009**, *11*, 3842–3845.

(8) (a) Screen, T. E. O.; Blake, I. M.; Rees, L. H.; Clegg, W.; Borwick, S. J.; Anderson, H. L. *J. Chem. Soc., Perkin Trans. 1* **2002**, 320–329. (b) Redmore, N. P.; Rubtsov, I. V.; Therien, M. J. *Inorg. Chem.* **2002**, *41*, 566–570. (c) Yoshida, N.; Ishizuka, T.; Yofu, K.; Murakami, M.; Miyasaka, H.; Okada, T.; Nagata, Y.; Itaya, A.; Cho, H. S.; Kim, D.; Osuka, A. *Chem.—Eur. J.* **2003**, *9*, 2854–2866. (d) Kamada, T.; Aratani, N.; Ikeda, T.; Shibata, N.; Higuchi, Y.; Wakamiya, A.; Yamaguchi, S.; Kim, K. S.; Yoon, Z. S.; Kim, D.; Osuka, A. *J. Am. Chem. Soc.* **2006**, *128*, 7670–7678. (e) Esdaile, L. J.; Jensen, P.; McMurtrie, J. C.; Arnold, D. P. *Angew. Chem., Int. Ed.* **2007**, *46*, 2090–2093. (f) Shen, D.-M.; Liu, C.; Chen, X.-G.; Chen, Q.-Y. *Synlett* **2009**, 6, 945–948. (g) Wallin, S.; Monnerau, C.; Blart, E.; Gankou, J.-R.; Odobel, F.; Hammarstrom, L. *J. Phys. Chem. A* **2010**, *114*, 1709–1721.

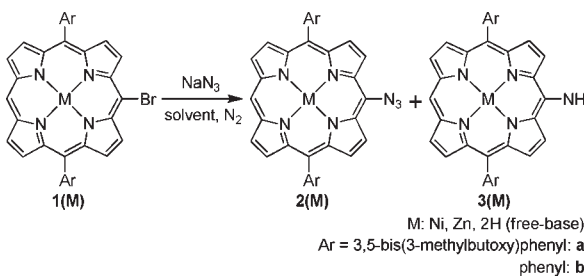
(9) Arnold, D. P.; Bott, R. C.; Eldridge, H.; Elms, F.; Smith, G.; Zojaji, M. *Aust. J. Chem.* **1997**, *50*, 495–503.

(10) (a) Bräse, S.; Gil, C.; Knepper, K.; Zimmermann, V. *Angew. Chem., Int. Ed.* **2005**, *44*, 5188–5240. (b) Chapyshev, S. V. *Synlett* **2009**, 1–8. (c) Minozzi, M.; Nanni, D.; Spagnolo, P. *Chem.—Eur. J.* **2009**, *15*, 7830–7840. (d) *Organic Azides: Syntheses and Applications*; Bräse, S., Banert, K., Eds.; John Wiley & Sons: Chichester, 2010.

(11) For *meso*-azidoporphyrins, see: (a) Smith, K. M.; Barnett, G. H.; Evans, B.; Martynenko, Z. *J. Am. Chem. Soc.* **1979**, *101*, 5953–5961. (b) Séverac, M.; Pleux, L. L.; Scarpaci, A.; Blart, E.; Odobel, F. *Tetrahedron Lett.* **2007**, *48*, 6518–6522.

(12) For  $\beta$ -azidoporphyrins, see: (a) Shen, D.-M.; Liu, C.; Chen, Q.-Y. *Eur. J. Org. Chem.* **2007**, 1419–1422. (b) Liu, H.; Duclairioir, F.; Fleury, B.; Dubois, L.; Chenavier, P. Y.; Marchon, J. C. *Dalton Trans.* **2009**, 3793–3799. (c) Lacerda, P. S. S.; Silva, A. M. G.; Tomé, A. C.; Neves, M. G. P. M. S.; Silva, A. M. S.; Cavaleiro, J. A. S.; Llamas-Saiz, A. L. *Angew. Chem., Int. Ed.* **2006**, *45*, 5487–5491.

**Table 1.** Catalyst-Free Aromatic Nucleophilic Substitution Reaction of *meso*-Bromoporphyrin **1(M)** with Sodium Azide<sup>a</sup>



entry	<b>1(M)</b>	solvent	temp (°C)	time (h)	yield <sup>b</sup> (%)	
					<b>2(M)</b>	<b>3(M)</b>
1	<b>1a(Ni)</b>	DMF	40	7	93	1
2	<b>1a(Ni)</b>	DMF	60	1	77	6
3	<b>1a(Ni)</b>	DMF	60	3	59	15 <sup>c</sup>
4	<b>1a(Ni)</b>	DMF	90	1.7	0	25 <sup>c</sup>
5 <sup>d</sup>	<b>1a(Ni)</b>	DMF	60	16.5	67	8
6	<b>1a(Ni)</b>	THF	60	2	0	0
7	<b>1b(Ni)</b>	DMF	40	16.5	68	12
8	<b>1a(Zn)</b>	DMF	90	18	0	trace <sup>e</sup>
9	<b>1a(2H)</b>	DMF	60	2.5	0	44 <sup>c</sup>
10	<b>1a(2H)</b>	DMF	60	0.5	23 <sup>f</sup>	39 <sup>f</sup>

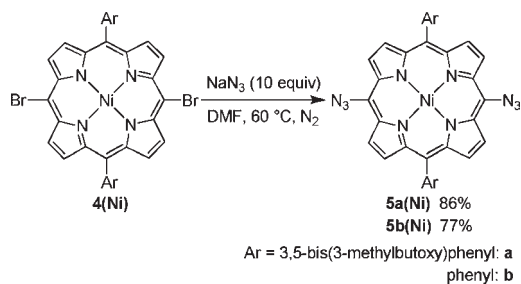
<sup>a</sup> Reaction condition: **1(M)** (10 mM), NaN<sub>3</sub> (10 equiv) under N<sub>2</sub> atmosphere with protection from light. <sup>b</sup> Isolated yields unless otherwise noted. <sup>c</sup> Undefined byproducts were also obtained. <sup>d</sup> 5 equiv of NaN<sub>3</sub>. <sup>e</sup> Recovery of **1a(Zn)**. <sup>f</sup> Yields were determined by the integral ratio of <sup>1</sup>H NMR of the crude products.

This reaction was also dependent on the central metal ion of the porphyrin. The reaction of zinc(II) complex **1a(Zn)** was significantly slower than that of **1a(Ni)**. Furthermore, we were not able to observe the formation of **2a(Zn)** at any stage in this reaction because of the harsh reaction conditions (Table 1, entry 8). This lower reactivity of **1a(Zn)** is attributed to the increase of the electron density on the porphyrin core induced by the electro-positive zinc(II) ion.<sup>1,6a</sup> In the case of free-base porphyrin **1a(2H)**, the main product was *meso*-aminoporphyrin **3a(2H)** after the complete disappearance of **1a(2H)** (entry 9). At an early stage in the reaction, free-base azidoporphyrin **2a(2H)** was detected by <sup>1</sup>H NMR and IR analyses of the crude reaction mixture but was not able to be isolated (entry 10). These results indicate that the substitution in **1a(2H)** proceeds slower than that in **1a(Ni)** while the thermal decomposition of the azide **2a(2H)** proceeds much faster than that of **2a(Ni)**. It is also noteworthy that the free-base *meso*-aminodiarylporphyrin is obtained directly from the corresponding *meso*-bromodiarylporphyrin in modest yield because *meso*-aminodiarylporphyrin has not been obtained directly by the reported procedures.<sup>9</sup>

To demonstrate the versatility of our procedure, the reaction of *meso*-dibromoporphyrin **4(Ni)** was performed to give *meso*-diazidoporphyrin **5(Ni)**. Indeed, treatment of *meso*-dibromoporphyrin **4a(Ni)** with 10 equiv of sodium

azide in DMF at 60 °C for 20 min gave the desired *meso*-diazidoporphyrin **5a(Ni)** in 86% yield (Scheme 1). We also examined the reaction of a Ni complex of  $\beta$ -bromotetraphenylporphyrin **6(Ni)** to evaluate the reactivity of  $\beta$ -positions. However, no substituted products were formed by treatment of **6(Ni)** with sodium azide at 90 °C for 18 h.

**Scheme 1.** Synthesis of *meso*-Diazidoporphyrin **5(Ni)**



Obtained *meso*-azidoporphyrins **2(Ni)** and **5(Ni)** are moderately stable at room temperature in the dark to perform structural analyses including NMR, MS, and X-ray analyses. By contrast, the photodecomposition of the azides proceeds gradually upon standing the dilute solution under room light (Figure S13). The <sup>1</sup>H NMR spectrum of **2a(Ni)** is almost identical to that of the reported one.<sup>11b</sup> IR spectra of **2a(Ni)** and **5a(Ni)** display intense characteristic stretching vibrations of the azide group at 2107 and 2105 cm<sup>-1</sup>, respectively (Figures S7–S8). The HR ESI-TOF MS spectrum of **2a(Ni)** clearly shows a expected molecular ion peak at 903.3966 for [**2a(Ni)**]<sup>+</sup> (Figures S3–S6). By contrast, the MALDI- or APCI-TOF MS spectrum of **2a(Ni)** does not show an expected molecular ion peak, but rather a peak corresponding to the nitrogen-eliminated ion [**2a(Ni)**–N<sub>2</sub>]<sup>+</sup>. UV–vis absorption spectra of **2a(Ni)** and **5a(Ni)** display typical Soret and Q bands of Ni(II) porphyrins (Figures S11–S12).

The crystal and molecular structures of **2b(Ni)** and **5b(Ni)** (Ar = phenyl) were determined by X-ray crystallographic analysis. The crystal structure of **2b(Ni)** is depicted in Figure 1. The porphyrin moiety is slightly ruffled with the average Ni–N(porphyrin) distance of 1.954 Å. The azido group is slightly tilted out of the porphyrin moiety with the C(1)–C(20)–N(5)–N(6) dihedral angle of 18.6(5)° because of the steric repulsion between the azide group and the neighboring  $\beta$ -hydrogen of the porphyrin. The closest contact distance between azide-N and  $\beta$ -H (N(6)⋯H(2)) is 2.37 Å, which is shorter than the sum of the van der Waals radii (1.55 Å + 1.20 Å = 2.75 Å).<sup>16</sup> The N(5)–N(6) bond length of 1.19 Å is significantly shorter than that of typical aryl azides (1.22–1.27 Å), while the N(6)–N(7) bond length of 1.16 Å is longer (1.11–1.14 Å).<sup>15</sup> In addition, the N(5)–N(6)–N(7) angle of 168.8(4)° is also slightly smaller than that of

(16) Bondi, A. J. *Phys. Chem.* **1964**, *68*, 441.



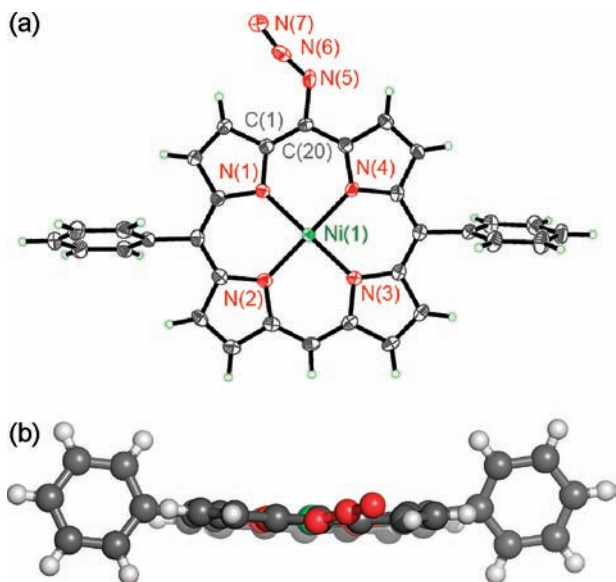


**Figure 1.** Crystal structure of **2b(Ni)**: (a) ORTEP view (50% probability), and (b) side view. Diffraction data were collected at  $-180\text{ }^{\circ}\text{C}$ . Selected bond lengths ( $\text{\AA}$ ) and angles ( $\text{deg}$ ): C(20)–N(5) 1.429(4), N(5)–N(6) 1.185(4), N(6)–N(7) 1.162(4), Ni(1)–N(1) 1.961(2), Ni(1)–N(2) 1.955(3), Ni(1)–N(3) 1.952(3), Ni(1)–N(4) 1.949(2), C(20)–N(5)–N(6) 124.9(3), N(5)–N(6)–N(7) 168.8(4).

the typical aryl azides ( $169^{\circ}$ – $174^{\circ}$ ).<sup>15</sup> Figure 2 displays the crystal structure of diazidoporphyrin **5b(Ni)**. The porphyrin moiety is more ruffled with the average Ni–N(porphyrin) distance of  $1.926\text{ \AA}$ . Two azide groups were crystallographically independent with different torsion angles of  $36.7(6)^{\circ}$  for **azide A** (N(5)–N(6)–N(7)) and  $67.6(5)^{\circ}$  for **azide B** (N(8)–N(9)–N(10)), respectively. The bond length and angle of **azide A** are similar to those of **2a(Ni)** while those of the **azide B** are rather similar to those of typical aryl azides. This difference might reflect the degree of the electronic  $\pi$ -conjugation between the porphyrin moiety and each azide group.

In summary, we have developed the facile synthesis of *meso*-mono- and diazidoporphyrins by the catalyst-free aromatic nucleophilic substitution of the corresponding *meso*-bromoporphyrins. The central metal ion of the

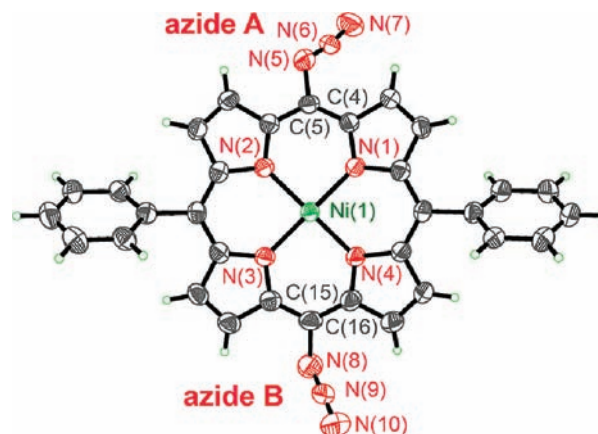


**Figure 2.** Crystal structure of **5b(Ni)** (ORTEP, 50% probability). Diffraction data were collected at  $-50\text{ }^{\circ}\text{C}$  because of the severe degradation of the diffraction at lower temperature. Selected bond lengths ( $\text{\AA}$ ) and angles ( $\text{deg}$ ): C(5)–N(5) 1.427(5), N(5)–N(6) 1.181(5), N(6)–N(7) 1.149(5), C(15)–N(8) 1.471(5), N(8)–N(9) 1.187(6), N(9)–N(10) 1.131(7), Ni(1)–N(1) 1.926(3), Ni(1)–N(2) 1.927(3), Ni(1)–N(3) 1.923(3), Ni(1)–N(4) 1.927(3), C(5)–N(5)–N(6) 121.5(3), N(5)–N(6)–N(7) 169.9(4), C(15)–N(8)–N(9) 115.9(4), N(8)–N(9)–N(10) 172.5(6).

porphyrin affects the reactivity of the porphyrin and the stability of the azides. In addition, the structure of the obtained azides has been determined by X-ray crystallographic analysis. X-ray analyses of large aromatic azides have been less reported despite their widespread synthetic use. Therefore, our unusual results have important significance in the chemistry of organic azides. Application of the azidoporphyrins based on the versatile reactivity of the azide group will be reported elsewhere. In addition, we are currently applying our procedure to the practical syntheses of various *meso*-heteroatom-substituted porphyrins.

**Supporting Information Available.** The experimental procedures, physical properties of new compounds, crystallographic data, and a CIF file for **2b(Ni)** and **5b(Ni)**. This material is available free of charge via the Internet at <http://pubs.acs.org>.